

# Numerical Investigation of Aspect Ratio Effect on Thermal Parameters in Laminar Nanofluid Flow in Microchannel Heat Sink

Seyed S. HOSSEINI<sup>1</sup>, Abbas. ABBASSI<sup>2</sup>

\* Corresponding author: Tel.: ++98 (21)64543425; Fax: ++98 (21)66619736; Email: [ssinahoseini@yahoo.com](mailto:ssinahoseini@yahoo.com)

<sup>1</sup> Faculty of Mechanical Engineering, University of Tehran, Iran

<sup>2</sup> Amirkabir University of Technology, Department of Mechanical Engineering, Iran

**Abstract** In this paper, laminar nanofluid flow of ethylene glycol-based of 4% volume fraction CuO(II) in a silicon rectangular microchannel heat sink with constant hydraulic diameter and different aspect ratios, with a constant heat flux, has been treated numerically. The effect of changing aspect ratios on the pressure loss and thermal parameters of the microchannel, such as Nusselt number(Nu), heat transfer coefficient(h) and non-dimensional temperature in fluid phase and solid(wall) phase have been investigated, using the finite volume method. In addition, the maximum and minimum values of thermal parameters and pressure loss have been calculated and the optimum aspect ratio for the performance of such systems has been evaluated.

**Keywords:** Nanofluid, Microchannel Heat Sink, Aspect Ratio, Thermal Parameter, Pressure Loss

## 1. Introduction

In order to cope with the ever increasing demands of various industries, such as aerospace and electronics, cooling devices have to be small, light and reliable in size, weight and performance .

The traditional and popular fluids used in heat exchangers like water, mineral oils and ethylene glycol play an important role in such industries. These fluids have limitations in transferring heat and cannot ensure rigorous performance, so they cannot satisfy the requirements of industry and solve its problems. Also, the size of the devices and equipment is continually decreasing and this means that heat transfer processes need improving and updating.

With the electronic industry's requirement for increasing heat transfer in limited spaces, conventional "extended surface" technology such as fins, have been unable to meet the demands [1].

Inspired by the microchannel heat-sink concept proposed by Tuckerman and Pease[1],

we propose combining this with the use of nanofluids in appropriate media. Because of its high potential to absorb heat, such an approach means that high heat fluxes can be transferred across these surfaces.

Experimental research at the micro dimensional level is complex and of high cost. This is especially so for the present case, in which several microchannels have to be made, and nano particles have to be produced for the nanofluids. Therefore numerical analysis can be a produced beneficial tool in this field.

Whether in the separate fields of microchannels and nanofluids, or combined in the studying the motion of nanofluids in microchannels, extensive investigations have been carried out.

Pease and Tuckerman [1] showed that their microchannel heat sink could accommodate a heat flux equal to  $790 \text{ W/cm}^2$ . Bowers and Mudawar [2] using a micro tube with a single phase flow of water, showed in their thermal experiments that, a heat flux of  $3000 \text{ W/cm}^2$  could be obtained.

Not only experimental investigations, but also many analytical studies have been made of heat transfer in microchannels. The so called fin analytical method- in which the solid part, separating two adjacent channels, is assumed to act as a fin-has been used in many researches.

Weisberg et al. [3] used a more real model addressing two dimensional and coupled heat transfer equations. This method included simulating the heat transfer in the fluid and the solid. Their main assumption was that, the flow is hydrodynamically and thermally fully developed. Viskanta and Fedrov [4] developed a three dimensional model for investigating heat transfer in microchannels, making the same assumption as Weisberg et al.

Despite the extensive experimental and analytical data obtained, areas of uncertainty remain. Various experimental studies have shown that fluid flow and heat transfer in microchannels, are different in behaviour from channels in macro dimensions. For the molecular case studied by Choi et al. [5] and Yu et al. [6] investigated the thermal and fluid flow characteristics for the special case of Nitrogen, gas and water, in different microtubes; they reported that the measured friction coefficient is less than the predicted values for their tubes of micro dimensions. The measured Nusselt number values were also greater than those predicted by the Dittus-Boelter correlation.

Peng and Peterson [7] studied single phase forced convection heat transfer using water. Their experimental channels were of rectangular cross section with hydraulic diameters ranging from  $133\mu\text{m}$  to  $367\mu\text{m}$ . Their results showed that the Reynolds number for the transition from laminar to turbulent flow is much smaller than for macro dimensions.

In order to ensure the benefits of micro channels are achieved and to further improve their performance, nanofluids are now being used. Nanofluids, a term introduced by Choi [8], represent a new class of engineered heat transfer fluids which contain metallic or carbon based particles with an average size of about 10nm. Nano particles, which present

appropriate thermal characteristics, are often spherical particles of aluminum and copper oxide with average size of 30 nanometers and volume concentrations of 0.001 to 6 percent. These particles, under static conditions, have generated elevated thermal conductivities [9-11].

Traditional theories, such as those of Maxwell or Hamilton and Crosser, cannot explain this nanofluid thermal phenomenon. Thus, new approaches and mathematical models involving new apparent (or effective) thermal conductivity have been proposed.

In this paper, to model the behaviour of nano particles in fluids, the model presented by Koo and Kleinstreuer [12] has been used. It has been derived experimentally and is in good agreement with experimental results. While  $h_{\text{fluid}}$  does not differ considerably from  $h_{\text{eff}}$ , when  $Pr > 1$ , the main improvement in heat transfer is attributed to  $h_{\text{eff}}$ .

Nevertheless, in this model a correlation is included for  $h_{\text{eff}}$ . The model posits that both  $h_{\text{eff}}$  and  $k_{\text{eff}}$  have two additive components, namely a static part ( $\mu_s, k_s$ ) and a dynamic part ( $\mu_{Br}, k_{Br}$ ), originating from the theory of Brownian motion of particles. An analytical solution for rectangular microchannels of different aspect ratios was undertaken by Lee and Garimella [13] in 2006. In that and other similar works, air and water were used as coolants. In our current study, ethylene glycol-based of 4% volume fraction CuO(II) is used as a nanofluid and flow is assumed laminar and fully developed. Also, the aspect ratio of the microchannel is varied. We have studied for the laminar flow regime, the variation of the average Nusselt number, and average convection heat transfer coefficient and pressure loss. Correlations are presented for these parameters enabling the minimum and maximum of these quantities to be calculated. Also, in the laminar flow regime, we have studied the effects of varying the aspect ratios of the microchannels upon the non dimensional temperature of the fluid phase and solid (wall) phase. The optimal aspect ratios are obtained for each individual effect and also overall..

## 2. Definition of Research Programme

### 2.1 Governing Equations

The heat sink investigated in this research is depicted in Fig. 1. Focusing on the microchannel shown in the center, the coolant, i.e., liquid plus nanoparticles, flows in the x-direction and the heat flux from the source,  $q''$ , caused via conduction. Assuming steady laminar flow of a dilute uniform suspension, and constant heat flux  $q''$ , the governing equations for this conjugate heat transfer problem are as follows:

- Continuity

$$\nabla \cdot \vec{u} = 0 \quad (1)$$

- Momentum equation

$$(\vec{u} \cdot \nabla) \vec{u} = -\frac{1}{\rho} \nabla p + \frac{\mu_{eff}}{\rho} \nabla^2 \vec{u} \quad (2)$$

- Energy equation for fluid

$$(\vec{u} \cdot \nabla) T = \frac{k_{eff}}{\rho c_p} \nabla^2 T + \frac{\mu_{eff}}{\rho c_p} \Phi \quad (3)$$

where

$$\Phi = \left( \frac{\partial u_i}{\partial x_j} + \frac{\partial u_j}{\partial x_i} \right) \frac{\partial u_i}{\partial x_j} \quad (4)$$

- Energy equation for solid

$$\nabla^2 T = 0 \quad (5)$$

- The boundary conditions are

$$u = U_0 \quad @ \quad x = 0 \quad (6)$$

$$\vec{u} = 0 \quad @ \quad \text{the wall} \quad (7)$$

$$\frac{\partial u}{\partial z} = 0 \quad @ \quad z = 0 \quad (8)$$

$$T_f = T_0 \quad @ \quad x = 0 \quad (9)$$

$$T_s = T_0 \quad @ \quad x = 0 \quad (10)$$

$$q'' = 0 \quad @ \quad x = 0, x = L, z = \frac{W}{2} \quad (11)$$

and  $y = H + t_0$

$$q'' = k_s \frac{\partial T}{\partial y} \quad @ \quad y = -t_0 \quad (12)$$

And at the wall-fluid interface we have

$$k_s \nabla T_s |_{n} = k_{eff} \nabla T_f |_{n} \quad (13)$$

As explained in the introduction, in the model used in this paper,  $k$  and  $\mu$  are composed of two parts, one static and the other dynamic, due to Brownian motion. (This has been validated by Koo & Kleinstreuer[12])

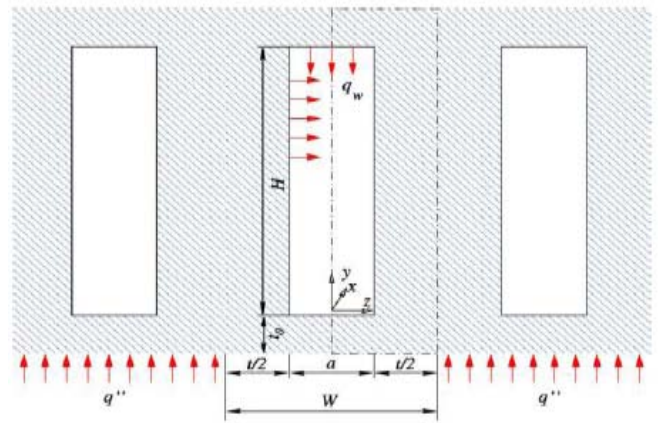


Fig. 1 Schematic of micro channel

The static part of the thermal conduction coefficient is defined by Maxwell as below [12]

$$\frac{k_{static}}{k_c} = 1 + \frac{3\left(\frac{k_d}{k_c} - 1\right)\alpha_d}{\left(\frac{k_d}{k_c} + 2\right) - \left(\frac{k_d}{k_c} - 1\right)\alpha_d} \quad (14)$$

In this equation,  $\alpha_d$  is the particle volume fraction,  $k_c$  is the thermal conductivity of the carrying fluid and  $k_d$  is the thermal conductivity of the particles.

The dynamic part resulting from Brownian motion is calculated using both Stoke's flow

approximation and kinetic energy theory [12]

$$k_{Brownian} = 5 \times 10^4 \beta \alpha_d \rho_l c_l \sqrt{\frac{\kappa T}{\rho_d D}} f(T, \alpha_d, etc.) \quad (15)$$

Functions  $\beta$  and  $f$  have been introduced to express respectively the hydrodynamic interaction among the Brownian motion induced fluid parcels, and the particle interaction due to its potential to encapsulate a strong temperature dependency. For  $\beta$  the following correlation is suggested.

$$\beta = 0.0137(100\alpha_d)^{-0.8229} \quad \alpha_d < 1\% \quad (16a)$$

$$\beta = 0.0011(100\alpha_d)^{-0.7272} \quad \alpha_d > 1\% \quad (16b)$$

For  $f$  experimental results show that the value “1” is acceptable to a very good approximation for the case which we have studied [12]. A correlation similar to  $k$  for fluid viscosity is available as follows

$$\mu_{Brownian} = \frac{k_{Brownian}}{k_l} \times \frac{\mu_l}{Pr_l} \quad (17)$$

## 2.2 Input data and assumptions

- The cooling of six different microchannels of constant hydrodynamic diameter (85.71 $\mu$ m) has been investigated. Average values have been obtained for ten surfaces from bottom to top of the channel.
- Aspect ratios investigated ranged between 0.16, for which experimental values were available, and 1, for which the cross section becomes symmetric.
- The wall material was silicon, and the depth of the channel was 1cm, to ensure fully developed flow.
- Inlet fluid temperature was 299K.
- The nanofluid, used was a 4% volume fraction of copper oxide (II) nanoparticles in ethylene glycol.

Nanofluids, containing either copper oxide nanoparticles or ethylene glycol, have proven to give high thermal performance in experimental studies.

•

Inlet velocity was taken as 2.2m/s which, given the constant hydraulic diameter condition, means the same Nusselt numbers.

## 2.3 Gridding

The standard gridding for both solid and fluid phases had a constant spacing of 10 $\mu$ m.

## 3. Solution method

### 3.1 Mathematical and numerical model

The continuity and Navier-Stokes equations with related boundary conditions were addressed, using a finite volume method. Thermal boundary conditions were: a constant heat flux of 100W/cm<sup>2</sup> and constant environment temperature. Laminar flow was assumed. The SIMPLE algorithm was used for coupling velocity and pressure during the multi grid solution. The momentum and energy equations were solved using second order upwind.

T

### 3.2 Validity of the solution

Since the available experimental data in the literature are in terms of local values of the parameters, it is not straightforward to verify the present results conclusively.. Nevertheless, we compared our results for an aspect ratio of 0.16, with published local experimental data. Data for the non dimensional fluid and solid temperatures (which will be introduced later), compares to within 20% approximately. This can be viewed as acceptable bearing in mind the differences above mentioned.

### 3.3 Grid independence

Grid independence has been investigated. With grid spacings half and twice the standard, the deviation of the results from the results for the standard grid was less than 1%. The results are given in Table 1.

Table 1 Comparison between the results of different grids

$y^*$ \ $\dot{\epsilon}_f$	Main interval-size grid	Half interval-size grid	2times interval-size grid
0	-0.42376	-0.42497	-0.42046
0.1	-1.52486	-1.52789	-1.52607
0.2	-1.98774	-1.98805	-1.98774
0.3	-2.09118	-2.08966	-2.09027
0.4	-2.1473	-2.14548	-2.14639
0.5	-2.19219	-2.19037	-2.19128
0.6	-2.22859	-2.22647	-2.22768
0.7	-2.25559	-2.25407	-2.25468
0.8	-2.26074	-2.26014	-2.26014
0.9	-2.11454	-2.11666	-2.11545
1.0	-1.07774	-1.07896	-1.07835

## 4. Results

### 4.1 Temperature profile

In this section the effect of varying aspect ratio on the temperature profile is discussed in terms of non dimensional temperature.

Non dimensional temperatures of the fluid and solid phases are defined as follows [12]

Solid phase:

$$\theta_s = \frac{\overline{T_s} - \overline{T_w}}{\frac{q_w H}{(1-\varepsilon)k_s}} \quad (18)$$

Fluid phase:

$$\theta_f = \frac{\overline{T_f} - \overline{T_w}}{\frac{q_w H}{(1-\varepsilon)k_s}} \quad (19)$$

All the variables are averaged in surfaces parallel with the heated surface.  $T_w$  is the average surface temperature at  $y=0$ .  $\overline{q_w}$  is defined in the following way:

$$\overline{q_w} = q'' \frac{W}{2(H+a)} \quad (20)$$

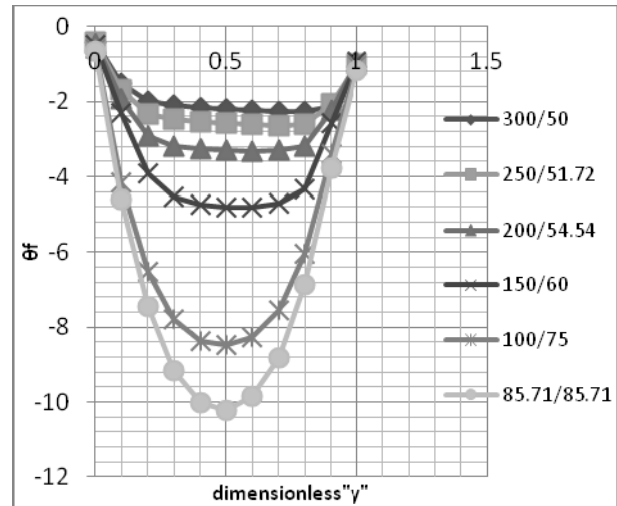


Fig. 2 Non dimensional fluid temperature in different sections

The  $y$  coordinate of the microchannel is also non-dimensionalised as follows:

$$y^* = y/H \quad (21)$$

Towards the center of the channel, the fluid temperature decreases while nearing the upper and lower surfaces, it increases. This phenomenon can be attributed to the solid phase which is in contact with the fluid. Higher temperatures arise at the lower surface, since the heat flux enters from that surface.

As the aspect ratio approaches 1, giving a more symmetric microchannel cross section, the fluid temperature decreases. For increasing aspect ratio, the cross section decreases, and with constant entrance velocity the mass flow entering is less. In addition, the area from which the heat flux enters is increased, whereas the entrance temperatures are the same; this shows poorer performance of the fluid in transferring heat.

By studying the solid phase non dimensional temperature, this becomes more evident.

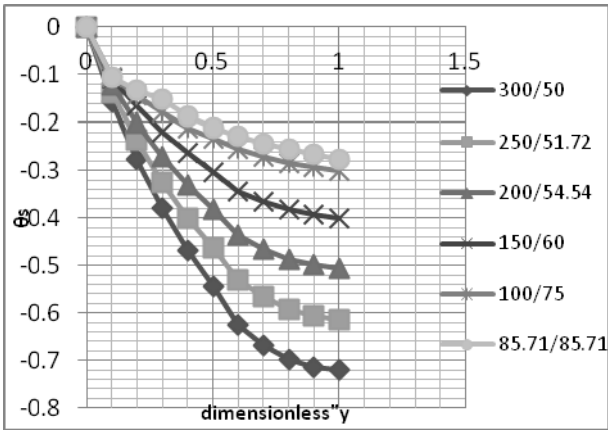


Fig. 3 Non dimensional solid temperature in different sections

It is seen in Fig. 3 that, for increasing symmetry of shape, the non dimensional temperature of the solid phase decreases, which indicates that this configuration is inappropriate. The heat transfer is also weak. These results are consistent with those of the fluid phase temperature.

#### 4.2 Pressure loss

The pressure loss is non-dimensionalized in terms of the pressure loss of the first aspect, and is defined as follows:

$$\hat{p} = \frac{P_{in} - P_{out}}{(P_{in} - P_{out})_{aspect\ ratio=0.16}} \quad (22)$$

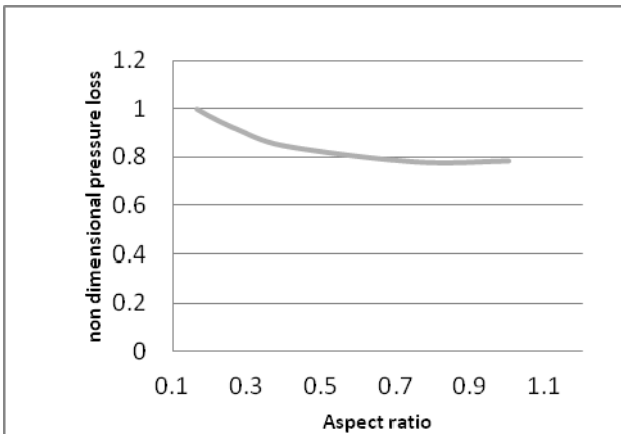


Fig. 4 Non dimensional pressure loss for different aspect ratios

In Fig. 4 the pressure loss is plotted versus the aspect ratio. It is seen that, as the aspect ratio increases, giving a cross section more nearly square in shape, the pressure loss decreases. For a fixed velocity and using the

static head loss relation,  $h_f = kv^2 / 2g$ , this pressure loss is logically defined. For increasing squareness of section, the head loss coefficient,  $k$ , decreases [14] and this is in good agreement with the results obtained. Therefore, from the pressure loss point of view, aspect ratios close to 1, are preferable.

#### 4.3 Nusselt number

The average Nusselt number ( $\overline{Nu} = \frac{\overline{h}D_h}{k_{eff}}$ ) has

also been studied for various aspect ratios.

The average heat transfer coefficient is calculated from the following relationship [12]

$$\overline{h} = \frac{\overline{q_w}}{\overline{T_w} - \overline{T_m}} \quad (23)$$

where  $\overline{q_w}$  is the same as introduced above.  $\overline{T_w}$ , is the wall ( $y=0$ ) average temperature and  $\overline{T_m}$ , is the fluid mean weighted average temperature. The axial conduction heat transfer in the microchannel, as defined, is justifiable to neglect [12].

Using the least square method, the best polynomial fitting the points obtained has been found. The resultant expressions for  $h$  and  $Nu$  are as follows:

$$h = 10^7 (1.2762\alpha^5 - 3.4812\alpha^4 + 3.5598\alpha^3 - 1.7090\alpha^2 + 0.3844\alpha - 0.0071) \quad (24)$$

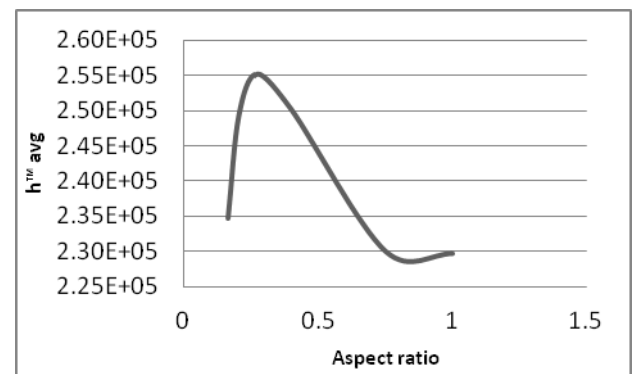


Fig. 5 Average Heat transfer coefficient in various aspect ratios

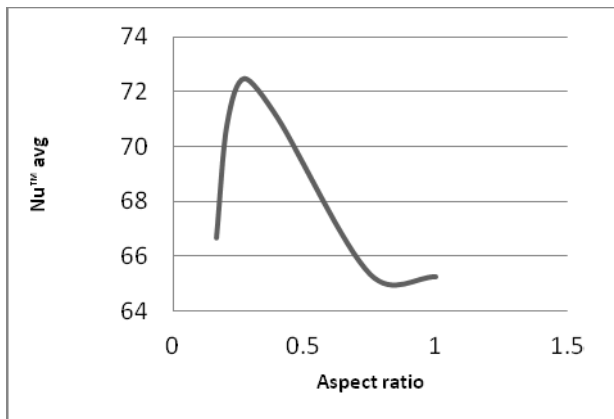


Fig. 6 Average Nusselt number in various aspect ratios

$$Nu = 3625\alpha^5 - 9888\alpha^4 + 10110\alpha^3 - 4854\alpha^2 + 1092\alpha - 20 \quad (25)$$

As is clear, both parameters that define the heat transfer have a maximum aspect ratio of  $\sim 0.3$  and a minimum  $\sim 0.9$ .

By considering temperature profiles, pressure loss, Nusselt number and heat transfer coefficient together it is concluded that for smaller aspect ratios, especially near 0.3, although the pressure is about 10% more than the symmetric configuration, the improvement in heat transfer under these conditions more than compensates for its weakness from the pressure loss point of view. ( $\sim 10\%$  more than for the symmetrical configuration)

## 5. Conclusions

Solid and fluid temperature profiles, pressure loss profile and average Nusselt number and average heat transfer coefficient profile of the laminar ethylene glycol-based nanofluid flow of a 4% volume fraction CuO (II) have been investigated for a silicon rectangular microchannel with constant hydraulic diameter and different aspect ratios. For such microchannels H1 thermal boundary conditions are used. The fluid flow is taken as

laminar, steady and fully developed. Numerical analysis, based on a finite volume method, has been performed to predict the heat transfer behaviour. General correlations have been developed for heat transfer coefficient and Nusselt number. The correlations presented are in a form suitable to predict the precise behaviour of the nanofluid.

## 6. References

- [1] D. Tuckerman, R. Pease, *High-Performance heat sinking for VLSI*, *IEEE Electron Dev. Lett. EDL-2* (5) (1981) 126-129.
- [2] I. Mudawar, M.B. Bowers, *Ultra-high critical heat flux(CHF) for Subcooled water flow boiling-I: CHF data and parametric effects for small diameter tubes*. *Int. J. heat and mass transfer* 42(1999)1405-1428.
- [3] A. Weisberg, H.H. Bau, J.N. Zemel, *Analysis of microchannels For integrated cooling*, *Int. J. Heat Mass transfer* 35(1992) 2465-2474.
- [4] A. G. Fedrov, R. Viskanta, *Three-dimensional conjugate heat transfer in microchannel heat sink for electronic packaging*, *Int. J. Heat transfer in micro tubes*, *ASME DSC* 40(1991) 89-93.
- [5] S. B. Choi, R. R. Barron, R.O. Warrington, *Fluid flow and heat transfer in micro tubes*, *ASME DSC* 40(1991) 89-93.
- [6] D. Yu, R. O. Warrington, R. R. Barron, T. Ameel, *An experimental and theoretical investigation of fluid flow and heat transfer in microtubes*, *ASME/JSME therm. Engineering*.
- [7] X. F. Peng, G. P. Pesterson, *convective*

*heat transfer and flow friction for water flow in microchannel structures, Int. J. heat mass transfer 39 (1996) 2599-2608.*

[8]S. Choi, *Enhancing thermal conductivity of fluids with nanoparticles, FED 231 (1995) 99-103.*

[9]S. Choi, Z. Zhang, W. Yu, F. Lockwood, E. Grulke, *Anomalous thermal conductivity enhancement in nano-tubes suspensions, Appl. Phys. Lett. 79 (14) (2001) 2252-2254.*

[10] J. Eastman, S. Choi, S. Li, W. Yu, L. Thompson, *Anomalous increased effective thermal conductivities of ethylene glycol-based nanofluids containing copper nano-particles, Appl. Phys. Lett. 78 (2001) 718-720.*

[11] H. Patel, S. Das, T. Sundararajan, A. Sreekumaran, B. George, T. Pradeep, *thermal conductivities of naked and monolayer protected metal nanoparticle based nanofluids: manifestations of anomalous enhancement and chemical effects, Appl. Phys. Lett. 83 (14) (2003) 2931-2933.*

[12]J. Koo, C. Kleinstreuer, *Laminar nanofluid flow in microheat-sinks, Int. J. Heat Mass transfer 48 (2005) 2652-2661.*

[13]Poh-Seng Lee, Sureh V. Garimella, *thermally developing flow and heat transfer in rectangular microchannels of different aspect ratios, Int. J. Heat and mass transfer 49 (2006) 3060-3073.*

[14]Erving H. Shames, *Fluid Dynamics.*